Advances in Science and Technology Research Journal

Advances in Science and Technology Research Journal, 2026, 20(2), 337–360
https://doi.org/10.12913/22998624/211734
ISSN 2299-8624, License CC-BY 4.0

Received: 2025.08.12
Accepted: 2025.12.15
Published: 2025.12.23

Testing of the sound level produced by a two-stroke piston internal combustion engine mounted on the aircraft depending on the propeller profile

Piotr Wróblewski[1,2*], Łukasz Kiszkowiak[2], Jarosław Milczarczyk[2], Przemysław Bratkowski[1,2]

[1] Faculty of Engineering, University of Technology and Economics H. Chodkowska in Warsaw, ul. Jagiellońska 82f, 03-301 Warsaw, Poland
[2] Faculty of Mechatronics, Armament and Aerospace, Military University of Technology, ul. Gen. Sylwestra Kaliskiego 2, 00-908 Warsaw, Poland
* Corresponding author's e-mail: piotr.wroblewski@wat.edu.pl

ABSTRACT

At present, two-stroke reciprocating internal combustion engines with a small total cylinder displacement are used to power ultralight aircraft. Their principal drawback is loud operation, particularly for operating and maximum values of the crankshaft rotational speed (RPM). The primary load on the powerplant is the propeller directly coupled to the engine crankshaft. This propeller – to a large extent – determines the characteristics of the sound level (acoustic signature) generated by the entire aircraft propulsion system. Additionally, the propeller blade airfoil itself generates additional aeroacoustic noise. Currently, engine designers pay a lot of attention to the sound level especially for civil aircraft, working near residential facilities or recreational areas. Tests were performed on a dedicated stand at a fixed distance. A simultaneous, dual-station setup was used—microphones in the propeller disk plane (L) and in the wake (T) - with thrust recording and five repeats per setpoint (A-weighted, FAST; energy-averaged means) for three 3-bladed CFRP propellers (Biela 32 × 12, Biela 32 × 14, Falcon 32 × 13) at 3000/4000/5000 RPM. Results show a monotonic rise in SPL with RPM and clear downstream directivity. At 5000 RPM, mean L(MAX) lies in 102.5–104.2 dB, while T(MAX) lies in 102.9–109.3 dB; mean thrust increases from ~111–147 N (3000 RPM) to ~323–405 N (5000 RPM). Biela 32 × 14 offers the most favorable thrust-to-noise trade-off (≈4.6 dB per 100 N). Practically, operating at ≤4000 RPM keeps mean maxima near ~102 dB at both positions for noise-sensitive missions. The innovativeness of the study consists in the simultaneous, dual-station noise measurement (in the propeller disk plane and in the downstream/wake direction) coupled with thrust recording and a full uncertainty budget, carried out on a dedicated test stand enabling stabilization of the shaft rotational speed and comparison of three propeller geometries.

Keywords: propeller noise, two-stroke piston aero engines, ultralight aircraft, propeller pitch and geometry, thrust–noise relationship.

INTRODUCTION

Contemporary research on aircraft noise emissions focuses on large powerplants, in particular on turboprop propulsion [1]. Recent NASA-led studies established baseline acoustic behaviors of small UAS, including component-level tonal/BPF content and strong configuration dependence, motivating standardized comparisons across propeller geometries [21, 22]. At present, aircraft propulsion is developing particularly rapidly in the use of advanced materials as well as internal combustion engines. In [13], the authors proposed employing a mechanism for forecasting the evolution of aeronautical structures within the multi-criteria design of the aircraft airframe geometry or the powerplant [13]. They proposed developing a system for analyzing the evolution

of parameters that are of primary importance to structural design. In this case, the main criterion becomes the requirement of the planned mission for the selected aircraft [13]. The more important parameters that should be taken into account in the design of new aircraft were presented in [14, 15]. In particular, the parameters of the propulsion system and the airframe during the takeoff and landing phases are important [15]. In [16], aerodynamic studies of aircraft were presented using the categories Very Light Aeroplane (VLA) and Very Light Jet (VLJ) as examples. In [16], the influence of the propulsion system on the aerodynamic characteristics of small aircraft was analyzed, primarily. Some simulation studies of small airplanes, as well as a presentation of the OSA aircraft fuselage, were presented in [17]. Meanwhile, [18] presented modern methods for designing and developing small aircraft in great detail. Against this background, recent sUAS acoustic surveys emphasize configuration-dependent tonal content and the need for harmonized test conditions when comparing propeller geometries [21, 23].

The research on aircraft noise emissions is particularly important in built-up areas within the aerodrome/airport environs. Human-response studies show that small-UAS noise tends to be perceived as particularly annoying due to prominent tones and temporal variability; psychoacoustic tests quantify these effects and inform suitable assessment metrics [22, 27].

In Poland, there are numerous legal acts concerning the measurement of noise emitted by aircraft. Likewise, the European Union has its own guidelines and regulations. The ICAO document in the area of noise emissions is Annex 16 – Environmental Protection, Volume I – Aircraft Noise. In framing quantities and instrumentation classes, the authors refer to ISO 1996-1 for environmental-noise descriptors and IEC 61672-1 for sound level meter performance classes (Class 1/2) [26, 28]. This volume introduces guidelines on permissible noise levels for various aircraft, noise-abatement procedures aimed at changing (reducing) the emitted noise level, and certification guidance [10]. Meanwhile, the European Union Aviation Safety Agency (EASA) has introduced Regulation (EC) No 216/2008 and Commission Regulation (EU) No 748/2012. The latter sets out the Type-Certificate Data Sheet for Noise (TCDSN), which contains measurement results for various types of engines, propellers, and mufflers/silencers, as well as weights, for different aircraft. These data are provided in detail in the EASA database. On the basis of ICAO Annex 16, Volume I, aircraft exempt from holding a noise certificate include aerobatic aeroplanes, motor gliders, and many others. In Poland, the Regulation of the Minister of the Environment of 16 June 2011 obliges airports to carry out acoustic measurements. These are general guidelines concerning aircraft and aerodromes.

In [11] it was noted that modifications to aircraft structures and new technologies in aviation lead to a reduction in generated noise levels. The results of studies on the noise emitted by turboprop- and turbofan-powered aircraft are presented in [2]. That work found that turbofan-powered aircraft emit the noise exceeding the applicable standards. In [2], measurements were conducted at the runway of Poznań-Ławica Airport. It was shown that the highest noise level and the greatest risk of exceeding permissible limits occur at the moment of take-off. Similar studies were conducted in [3], where the negative effects of excessive aircraft noise were indicated. The impact of noise emitted by small aircraft on people was analyzed in [9]. These studies concerned large aircraft powerplants. Nevertheless, there are few scientific studies concerning small aircraft, in particular two-stroke piston internal combustion engines. The research on the possibility of reducing the noise level in small aircraft was analyzed in [4]. In these studies, it was found that, in order to reduce the maximum noise level, it is necessary to lower propeller blade tip speed. Two-stroke piston internal combustion engines intended for the propulsion of small aircraft are used in recreational/sport aviation and in small aircraft intended for aerobatic flight. These engines have been only sparsely investigated with respect to the generated sound level, especially under various engine operating conditions and with different propeller geometries. Such investigations are also valuable from a diagnostic standpoint in order to determine engine operating characteristics under varying load. Under aircraft flight conditions, such studies should be carried out in accordance with the applicable regulations in the given territory.

At present, propeller propulsion in large aircraft has been partially displaced by large turboprop and turbofan engines. Thrust is to a large extent dependent on the propeller blade airfoil/profile, which in turn leads to varying values of the noise level emitted by the powerplant. Research on propeller aerodynamics was conducted in [5].

That work considered the influence of propeller profiles on the thrust produced by the powerplant. The operational parameters of a reciprocating internal-combustion engine were also investigated in [19], where the primary focus was the influence of lubricating oils on engine performance. Engine-borne contributions are also configuration-dependent; intake-system flow stability under throttling highlights how induction hardware and operating point can alter the propulsion acoustic signature [34]. The impact of the propeller blade profile on emitted noise and its effect on the surroundings was studied in [6]. It was stated that the harmonic components depend on the number of blades and the rotor speed. Similar studies were analyzed in [7, 8]. Foundational airfoil self-noise research explains the broadband mechanisms (e.g., turbulent boundary-layer–trailing-edge noise) that, together with BPF tones, shape small-propeller signatures [29]. CFD-based rotor parameterization across flight conditions underscores the sensitivity of tonal and broadband content to inflow angle, advance ratio, and operating point, reinforcing the need for harmonized comparisons when evaluating propeller geometries [33].

Wind-tunnel acoustic data can also be leveraged to simulate sUAS flyover noise for human-response studies, supporting consistent cross-scenario comparisons [30]. Complementary gust-modeling studies using state-of-the-art CFD for small UAVs quantify the impact of unsteady inflow on blade loading and tonal BPF content, helping translate static-stand observations to flight conditions [31]. Parametric analyses indicate that even modest variations in gust angle and velocity can shift surface-pressure features (e.g., stagnation position), altering the unsteady loading that feeds propeller noise mechanisms [32]. These investigations were conducted experimentally using sound level meters. The test methodology varied, in particular, different stand-off distances from the test article were adopted. In this case, the tests concerned electrically powered drones (UAS/UAV). There is a lack of broader research on sound level measurements for two-stroke piston internal-combustion engines. Field-measurement frameworks for multirotor UAS now enable comparable LAmax/LAE metrics, directivity maps, and source-hemisphere reconstructions in outdoor operations [24]. Comparative on-site studies further link measured noise to perceived annoyance across platforms and maneuvers, underscoring operational relevance [25]. Therefore, there is a reasonable need to examine the noise level (sound pressure level – SPL) for a two-stroke piston internal combustion engine depending to the type of propeller and the engine crankshaft speed. Such research is carried out in a specially built research stand using various propeller profiles. The novelty is to conduct research for various engine parameters and propellers in a specially prepared position. In addition, the appropriate way of placing the sensor of the emitted noise level was adopted. The conclusions of these studies are a source of information on the selection of propellers for the parameters of the piston internal combustion engine. This is especially important when using this type of drive for ultralight aircraft performing operations near people inhabited by people. In addition, the emitted noise can also be additional information on the course of the operation of the power unit. Studies of the level of emitted noise for small engines, especially using dedicated research stations, are sporadically conducted mainly by engine manufacturers to a very limited extent.

In recent years, the number of light manned and unmanned aircraft conducting recreational, sport, and specialized missions (infrastructure monitoring, photogrammetry, medical transport) has increased significantly. The growing density of flight operations below 300 m AGL results in local communities increasingly filing complaints about excessive noise, especially in suburban areas and environmentally protected areas. Above ground level (AGL) is the altitude measured above the terrain directly beneath the aircraft. This trend has also been presented in detail in the EU U-space framework (Regulations (EU) 2021/664, 2021/665, and 2021/666). These regulations present environmental requirements for unmanned aircraft systems (UAS). This opens new research perspectives related to acoustic (noise) certification of aircraft with a maximum take-off mass (MTOM) below 25 kg. At present, for this type of aircraft there is no clear, unified system for assessing the generated noise.

The propeller on an aircraft generates thrust and constitutes the primary source of noise. Both of these parameters result from the forced circulation of air around the rotating propeller blades. Any modification of geometry or change in rotational speed (RPM) that increases the pressure differential between the pressure side and the suction side increases thrust. At the same time, this affects the two main components of the acoustic

spectrum: loading noise, which depends primarily on the pressure distribution over the blade surface; and tip noise as well as wake/vortex noise behind the propeller disk, which depend on the local Mach number at the blade tip. This noise scales with the third power of rotational speed and diameter [29].

In two- and three-bladed propellers, power absorption is distributed differently. This affects the formation of different acoustic characteristics (signature). Two-blade propellers carry higher unit blade loading. Three-blade propellers reduce the load on each individual blade. For the same shaft power, it is therefore possible to obtain similar or greater thrust at a lower maximum generated noise level. The investigations in this work focused mainly on the three-bladed propellers made of carbon-fiber composite (CFRP). Propeller diameter directly affects the propeller disk area and blade tip speed. A larger diameter enables the same thrust to be produced with a smaller change in jet/wake velocity, which reduces blade-tip noise. Longer propeller blades generate low-frequency pressure waves of higher amplitude. In this case, it should be recognized that propeller geometry alone has a very strong influence on the generated thrust and on the maximum noise level. It also causes variation in the noise frequency content. Such noise can be burdensome for aircraft operators.

The geometric pitch of the propeller strongly affects the effective angle of attack. A larger pitch reduces the required engine shaft RPM, which allows the fundamental tone (blade-passage frequency – BPF) responsible for annoying noise to be lowered. Unfortunately, with excessively high pitch values this can lead to an increase in broadband turbulent noise (BBN). These relationships are strongly nonlinear. Fully illustrating this state requires experiments covering a wide range of propeller pitch configurations. Model studies are not very accurate due to the numerous variables that significantly influence the final result. Therefore, in such research, experimental testing is recommended.

On a two-stroke piston engine installed on the OSA 3 aircraft, three propeller pitch settings were tested for three-bladed carbon-fiber (CFRP) propellers. In this way, thrust and noise level characteristics were obtained for ultralight aircraft. The novelty of this work is the combined measurement of thrust and sound level on a purpose-built test stand/rig. This stand was custom-built specifically for these studies. In particular, the engine installation on the fuselage and the test method itself make it possible to obtain reliable results.

The literature does not sufficiently describe the comprehensive influence of blade geometry (pitch, airfoil/profile) and crankshaft rotational speed on sound level across the operational envelope at typical crankshaft speeds. Few studies have been published on two-stroke aero engines. Recent work [20] has investigated the influence of propeller blade profile, angle of attack, and the number of blades on the performance parameters of a two-stroke aero engine, confirming that propeller geometry directly affects thrust, shaft rotational speed, and engine thermal load. The study highlighted that there is no universal propeller ensuring both maximum thrust and low thermal stress, and emphasized the importance of experimental bench tests to identify the optimal propeller configuration. The research conducted in this article partially bridges this gap by combining the prescribed test conditions with the ability for precise adjustment of engine parameters and interchangeable propeller sets. Highly precise control and actuation instrumentation ensures high control accuracy. The analysis presented couples two parameters, i.e. the required thrust and noise constraints, within a single test campaign. This enables the selection of a propulsion system for ultralight aircraft operating near populated areas. This is particularly important in the case of combat drones (UAS) intended for military use.

RESEARCH METHODOLOGY

Construction and more important elements of the research position

The test stand for propeller and sound level measurements was built on the basis of the OSA 3 aircraft. A special load-bearing frame was attached to the aircraft fuselage, onto which the tested piston internal-combustion engine was mounted (Figure 1). A two-stroke engine 3W-275Xi B2R TS CS was installed on the aircraft. The OSA 3 fuselage was mounted on tricycle landing gear. The research stand was designed to enable precise testing of two-stroke piston aero engines. Flight tests under actual flight conditions are also planned. The engine and powerplant arrangement allows the installation of various two- and three-bladed propellers

of different diameters. The OSA 3 test rig design enables measurement of numerous engine operating parameters and the integrated propeller. In this work, extensive development was carried out on remotely operated measurement systems. The bench tests include recording thrust, cylinder-head temperatures (CHT), vibration signals, and acoustic emission level (SPL). An important element of the OSA 3 stand is an advanced measurement chain built with Futaba FASSTest and T-FHSS Air devices, which provides monitoring of all operating parameters of the reciprocating internal-combustion engine. A CL14 load cell was used to measure thrust, capable of measuring tensile and compressive forces. Measurement is possible over a 0–5 kHz frequency range with accuracy $\leq 0.5\%$ [12]. In the experiment, these measurements were used to generate thrust characteristics as a function of shaft rotational speed and propeller geometry, which enabled comparison of noise levels between propeller profiles at identical shaft RPM and analysis of the thrust–noise relationship.

It is worth noting that each propeller type, operating with the same engine, allows a different value of maximum thrust and maximum crankshaft RPM to be achieved. The CL14 load cell works with the single-channel CL450 data logger, the temperature coefficient of which is $\leq$ 0.05%/10 K [12]. A test stand built in this way makes it possible to obtain the appropriate measurements necessary for validation of numerical models of propeller noise and for the selection/tuning of operating parameters of two-stroke piston engines used in light and UAS.

In Figure 1, the placement of the force sensor (load cell) can be seen, suspended on dedicated straps/slings and anchored to the ground using special fittings/connectors. Such positioning of the measuring element allows the thrust force generated by the propulsion system (powerplant) to be determined directly. In this case, there is no need to apply correction factors, as is required with the test stands employing a load-bearing frame [12]. The only requirement is the proper parallel alignment of the sensor straps with the engine axis of the unit installed on the aircraft (Figure 2).

In the tests, an auxiliary cooling system was implemented using a QX-MOTOR 64 mm EDF (Electric Ducted Fan) with a QF2822(2222)-3500 KV motor, powered by a 4S LiPo battery (14.8 V). Fan control and speed regulation are performed remotely via in-house (proprietary) software. The principal parameter subject to adjustment is the rotational speed of the fans (RPM). The fans are shown in Figures 3 and 4.

No deflectors or screens were used. The study targeted the natural propeller slipstream to preserve repeatable, comparable conditions representative of operational use. The influence of nearby walls was assessed as minor for the adopted geometry; differences in SPL remained within the combined uncertainty band. For safety, thrust anchoring was installed at the rear of the laboratory. A follow-on campaign on an airfield apron with mobile anchoring and optional wind screens is planned to quantify any residual enclosure effects.

Abatronic AB-8852 (gray) is a Class 2 sound level meter compliant with international standard IEC 61672-1. The instrument is equipped with a

Figure 1. View of the OSA 3 aircraft with the 3W-275Xi B2R TS CS engine and tailplane

Figure 2. View of the load cell installation and the layout of test subsystems during thrust testing and noise-level measurement

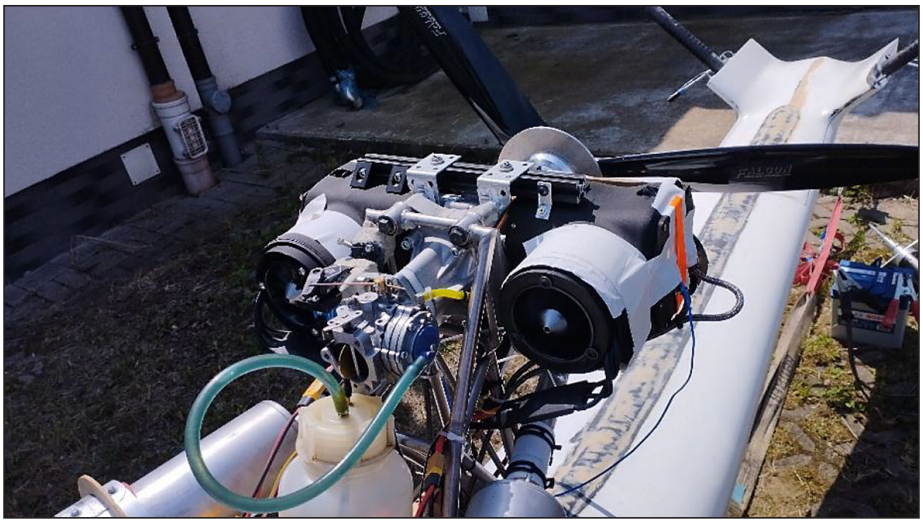

Figure 3. View of the cooling fans with custom-built air ducts

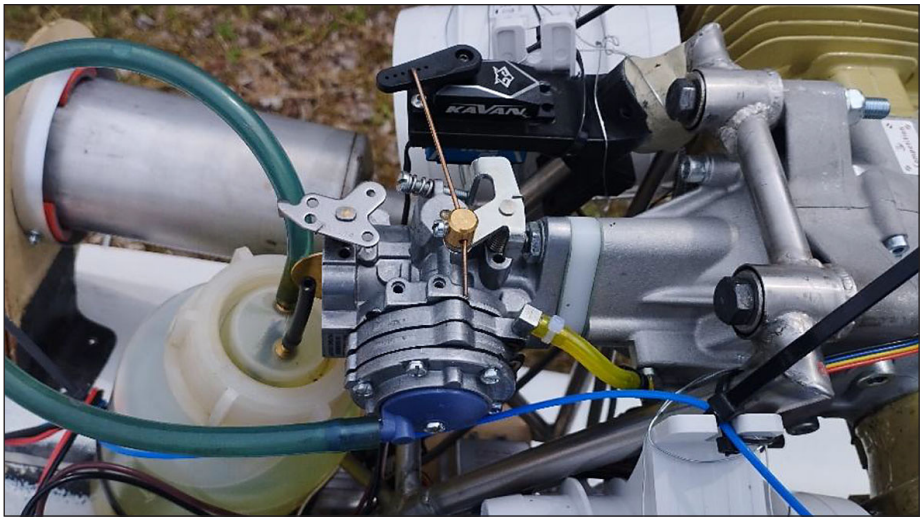

Figure 4. View of the fuel supply system

four-digit, backlit LCD with 0.1 dB resolution, updated twice per second, and its measurement range is 30 to 130 dB with high accuracy of ±1.4 dB. Three manually selectable sub-ranges – low (30–80 dB), medium (50–100 dB), and high (65–130 dB) are complemented by an AUTO mode covering the full 30–130 dB span.

The meter supports two time weightings: FAST (time constant 125 ms) and SLOW (1 s), as well as two frequency weightings, A and C. A ½″ electrostatic microphone records sounds over the 31.5 Hz to 8 kHz band with a 50 dB dynamic range. Calibration is facilitated by a dedicated port, and the AC/DC analog output (AC = 1 V rms, DC = 10 mV/dB) plus a 3.5 mm headphone jack enable further signal processing. AB-8852 operates under conditions of 0 to 40 °C and 10 to 90% RH. In the tests, to measure the temperature in the vicinity of the cylinder heads, in contact with the base material, a Type K thermocouple FTARB04-K-M5P2 was used, designed for mounting with an M5 screw. The sensors have a measurement accuracy of ±0.75%·t for Types K and J. The sensors have good insulation resistance of 5 MΩ at 20 °C and relative humidity below 80% [12]. A MAX6675 converter was used with the thermocouple; it performs digital conversion of the temperature signal over 0–1024 °C with 0.25 °C resolution. The MAX6675 provides a 12-bit SPI digital output, and its measurement error is at most 8 LSB over 0–700 °C. The converter is characterized by current consumption of 0.7–1.5 mA, high noise immunity, and built-in open-circuit detection. The conversion time is approximately 220 ms [12].

The Abatronic AB-8852 sound level meter was used in two measurement positions. Position L (propeller disk plane): the microphone was placed 3 m from the propeller axis, in the plane of the propeller disk, at the height of the propeller hub. Position T (aft of the aircraft): the same meter was set 1 m behind the tail (i.e. 2.6 m aft of the propeller) and 1 m to the left of the propeller axis, at the same height as in position L. For each test variant and propeller type, measurements at positions L and T were carried out under identical ambient conditions at crankshaft rotational speeds of 3000, 4000, and 5000 RPM. For reference, the thrust characteristics are presented for ±100 RPM around each setpoint. Thus Type-B uncertainty is the same in L and T. All sound pressure level (SPL) measurements were performed five times at the same crankshaft rotational speeds, with a start-of-measurement temperature of approximately 50 °C, relative humidity of 40%, and ambient temperature of 26 °C. The tests were conducted at different time intervals with continuous logging of thrust and temperature. Readout from the sound level meter was performed manually by latching/freezing the minimum and maximum SPL values for each measurement variant. This activity was carried out by two operators simultaneously, while a third operator remotely controlled engine operation, achieving the target RPM and thrust.

Acoustic measurement parameters and rationale. SPL was recorded as A-weighted levels with FAST time weighting (125 ms) to reflect human loudness perception and to capture short-time extrema during steady operation. For each test point, the MIN and MAX SPL values were latched over a ~10 s window and repeated the procedure five times (n=5). A-weighting was selected because it is the de-facto standard for environmental/operational aircraft noise, while FAST weighting better represents momentary peaks than SLOW. Mean levels were computed in the energy domain (Equation 1); Type-A and Type-B components were combined into the combined standard uncertainty (Equations 3–6). All measurements were taken with the same meter (Abatronic AB-8852; accuracy ±1.4 dB), hence $u_B(T) = 1.4/\sqrt{3} = 0.81$ dB at both positions L and T. The average SPL is calculated on an energy (logarithmic) scale [35]:

$$\bar{L}_E = 10\log_{10}\left(\frac{1}{n}\sum_{i=1}^{n} 10^{L_i/10}\right) \quad (1)$$

where: $\bar{L}_E$ – energy (logarithmic) mean sound level [dB], L_i – sound level of the i -th repetition in the series [dB], n – number of repetitions (measurements) in the series, $\log_{10}(\cdot)$ – base-10 logarithm, $10^{Li/10}$ – conversion of a level in dB to a linear (energy/power) ratio.

Arithmetic average (only comparative) [35]:

$$\bar{L}_A = \frac{1}{n}\sum_{i=1}^{n} L_i \quad (2)$$

where: $\bar{L}_A$ – arithmetic mean sound level [dB]; L_i – sound level of the i-th repetition [dB]; n – number of repetitions.

For the considered series, the differences between $\bar{L}_E$ and $\bar{L}_A$ are in the order of 0.03–0.10 dB, so the average values of the tables can remain (rounded to 0.1 dB). Standard deviation of the series (for repetitions) [36, 37]:

$$s = \sqrt{\frac{1}{n-1}\sum_{i=1}^{n}(L_i - \bar{L}_E)^2} \quad (3)$$

where: s – sample standard deviation of the series [dB].

Average A uncertainty (standard medium error) [36, 37]:

$$u_A = \frac{s}{\sqrt{n}} \quad (4)$$

where: u_A – type A standard uncertainty of the mean (repeatability) [dB].

Type B uncertainty from the meter (rectangular distribution) [36, 37]:

$$u_B = \frac{a}{\sqrt{3}} = \frac{1.4}{\sqrt{3}} = 0.81 \text{ dB} \quad (5)$$

where: u_B – type B standard uncertainty due to instrument accuracy [dB], a is the manufacturer's accuracy [db].

For Abatronic AB-8852 $a = \pm 1.4$ dB $\Rightarrow u_B = \frac{1.4}{\sqrt{3}} = 0.81$ dB.

Complex standard uncertainty [36, 37]:

$$u_c = \sqrt{u_A^2 + u_B^2} \quad (6)$$

where: u_c – combined standard uncertainty of the mean result [dB].

General notes

- All levels are sound pressure levels expressed in decibels (dB).
- The energy mean $\bar{L}_E$ uses the physically correct energy domain; the arithmetic mean may be shown only for comparison.

Throughout the test campaign, cylinder-head temperature (CHT) was monitored; in the case of the second cylinder head, it was slightly higher. Measurements were halted at a temperature of about 100 °C. Owing to the use of additional high-power fans, the engine did not undergo excessive overheating. Fan throughput/output was regulated remotely and set appropriately to the engine operating conditions and external conditions.

RESEARCH RESULTS AND DISCUSSION

Sound level measurement for the Biela 32×12 three-bladed carbon-fiber propeller

The sound level (SPL) measurements for the Biela 32 × 12 propeller were performed for three shaft speeds (3000, 4000 and 5000 RPM). These measurements have been included in a detailed analysis of both minimum and maximum levels of noise registered by an Abatronic AB-8852 sound level meter (Figures 5–7). The analysis clearly indicates an increase in sound level as the propeller RPM increases. Both the minimum and maximum values registered at both measurement positions (L and T) clearly grow in subsequent ranges of the crankshaft. A clear upward trend is evident in all cases. Raising RPM from 3000 to

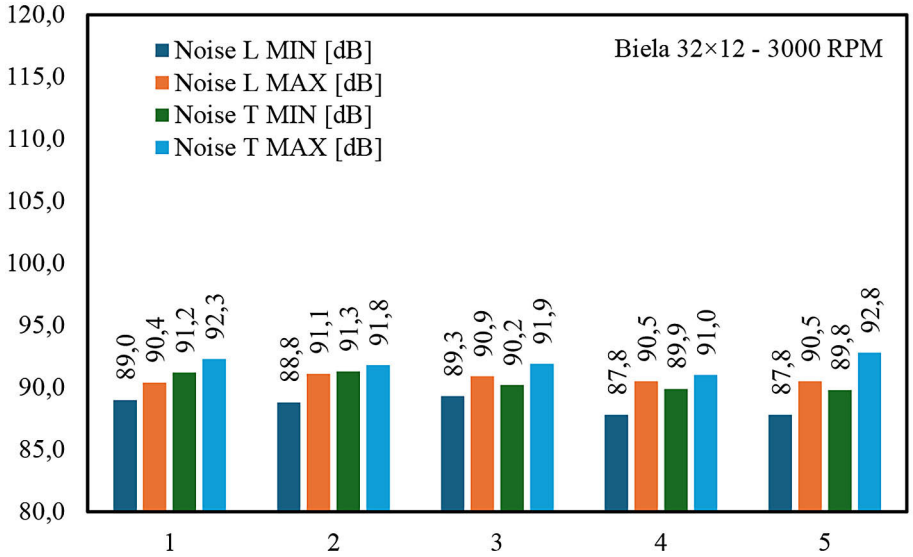

Figure 5. Sound level measurement – minimum and maximum values for the powerplant equipped with the Biela 32 × 12 propeller, recorded at positions L and T with the Abatronic AB-8852 at 3000 RPM

5000 increases the noise level by 12.2 dB (L MIN) and 11.8 dB (L MAX); at position T, the increase is 7.3 dB (T MIN) and 12.5 dB (T MAX). This shows that the noise emitted by the Biela 32 × 12 propeller depends strongly on rotational speed. Across all RPM settings, measurement repeatability is high. The Type-A standard uncertainty of the mean is below 0.4 dB in most cases (the sample standard deviation s is typically < 1 dB). The results indicate that, at higher RPM, the Biela 32 × 12 produces the noise levels that may be significant for hearing protection and user comfort. Values above 100 dB (at 5000 RPM) may pose a health risk under prolonged exposure (Figure 7). On all SPL figures, the data correspond to two microphone positions measured with the same sound level meter (Abatronic AB-8852): L – propeller-disk plane (microphone 3 m from the propeller axis, at hub height); T – aft of the aircraft (microphone 1 m behind the tail, i.e., 2.6 m aft of the propeller, and 1 m to the left of the propeller axis, at the same height as in L).

On the basis of the technical data from the meters and the measurement error values, the total measurement uncertainty was determined using the formula for the combined standard uncertainty of Type A and Type B (Table 1):

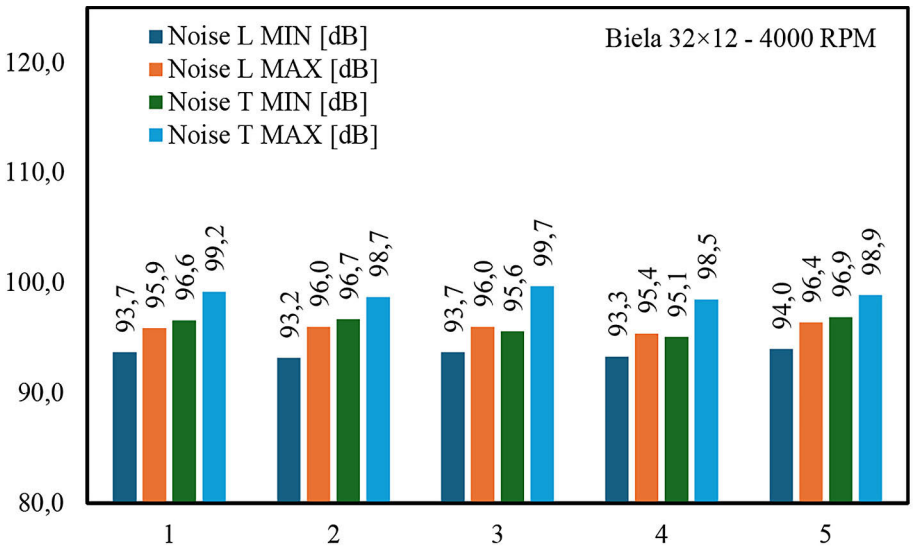

Figure 6. Sound level measurement – minimum and maximum values for the powerplant equipped with the Biela 32 × 12 propeller, recorded at positions L and T with the Abatronic AB-8852 at 4000 RPM

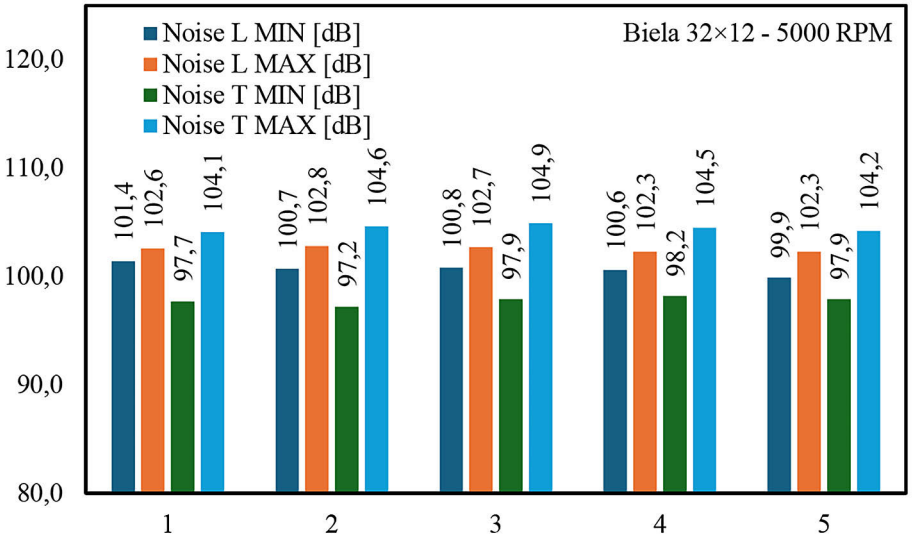

Figure 7. Sound level measurement—minimum and maximum values for the powerplant equipped with the Biela 32 × 12 propeller, recorded at positions L and T with the Abatronic AB-8852 at 5000 RPM

During the tests conducted for the Biela 32 × 12 propeller, the thrust generated by the propeller and the temperatures at both cylinder heads were recorded in parallel with the noise measurements. Figure 8 shows the time history of thrust generated by the Biela 32 × 12 propeller at 3000 RPM for the 3W-275Xi B2R TS CS engine. The dataset comprises 597 measurements. The number of samples resulted from the test duration and the time for which the rotational speed was maintained; this value varies for each primary test point. The presented RPM range is 2900–3100 RPM. The arithmetic mean thrust for this range was 111.01 N. As it can be observed, the thrust value is fairly stable around 3000 RPM, which does not disturb the obtained acoustic measurement results. Small, random deviations are visible typical of dynamic measurements of this type – however, the overall trend shows no significant anomalies. Thrust stability indicates correct operation of both the powerplant

Table 1. Results of measurement error and uncertainty calculations for the Biela 32 × 12 propeller

Results for the Biela 32 × 12 propeller – 3000 RPM				
Measurement type	Mean value	Measurement error / Type A uncertainty u_A [dB]	Type B uncertainty u_B [dB]	Combined uncertainty u_C [dB]
Noise L MIN	88.5	0.31	0.81	0.87
Noise L MAX	90.7	0.14	0.81	0.82
Noise T MIN	90.5	0.32	0.81	0.87
Noise T MAX	92.0	0.30	0.81	0.86
Results for the Biela 32 × 12 propeller – 4000 RPM				
Measurement type	Mean value	Measurement error / Type A uncertainty u_A [dB]	Type B uncertainty u_B [dB]	Combined uncertainty u_C [dB]
Noise L MIN	93.6	0.15	0.81	0.82
Noise L MAX	95.9	0.16	0.81	0.83
Noise T MIN	96.2	0.35	0.81	0.88
Noise T MAX	99.0	0.21	0.81	0.84
Results for the Biela 32 × 12 propeller – 5000 RPM				
Measurement type	Mean value	Measurement error / Type A uncertainty u_A [dB]	Type B uncertainty u_B [dB]	Combined uncertainty u_C [dB]
Noise L MIN	100.7	0.24	0.81	0.84
Noise L MAX	102.5	0.10	0.81	0.82
Noise T MIN	97.8	0.17	0.81	0.83
Noise T MAX	104.5	0.14	0.81	0.82

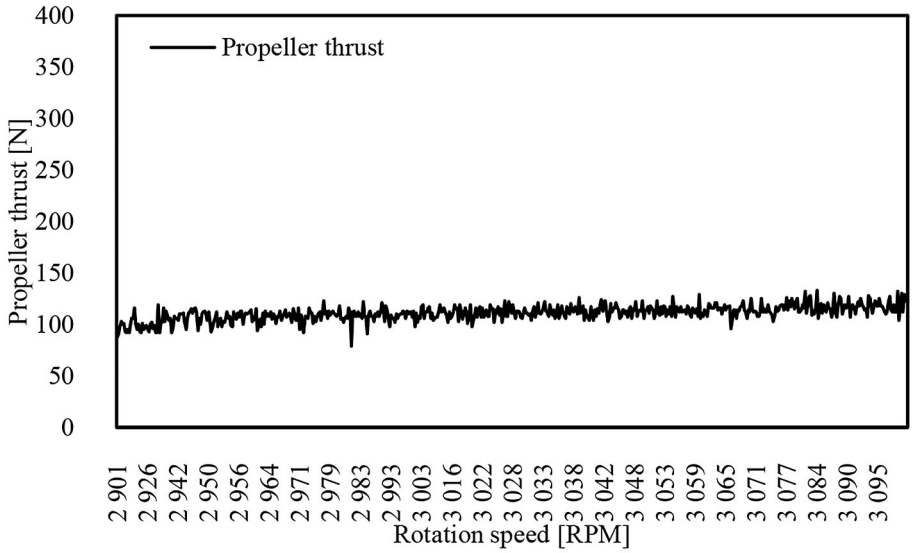

Figure 8. Thrust characteristic of the Biela 32 × 12 propeller for the 2900–3100 RPM range

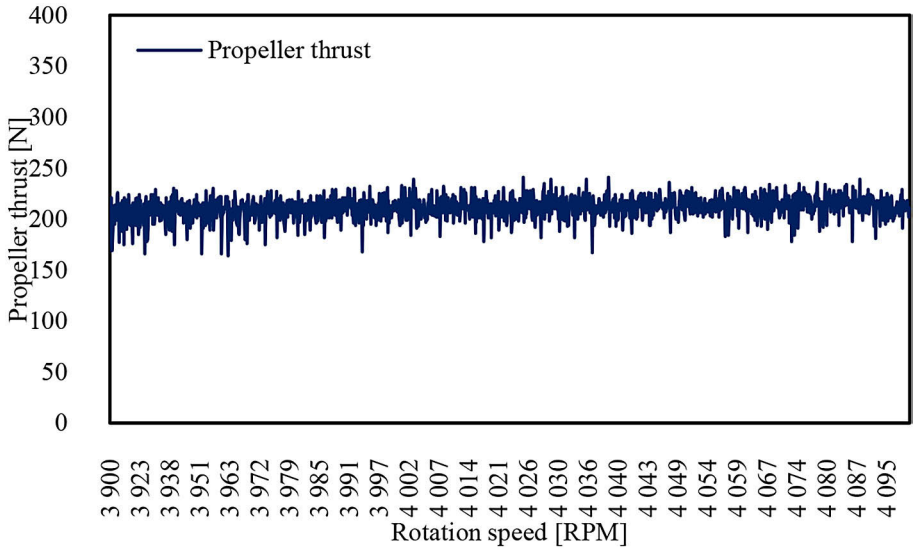

Figure 9. Thrust characteristic of the Biela 32 × 12 propeller for the 3900–4100 RPM range

and the propeller itself, as well as ensures repeatable conditions for the concurrent sound level measurements. The slight increase in thrust at the upper end of the range (above 3050 RPM) suggests the natural rise in force with increasing RPM consistent with propeller operating characteristics. Across the entire examined range there are no thrust spikes or drops that would indicate instability of the propulsion system or propeller design defects. Constant thrust at constant crankshaft speed is essential for obtaining comparable measurement data, as it eliminates the influence of random fluctuations in engine operation. Similar datasets were compiled for 4000 RPM and 5000 RPM.

Figure 9 presents the time history of thrust generated by the Biela 32 × 12 propeller over the rotational-speed range of approximately 3900 to 4100 RPM. This range corresponds to the next propeller operating level analyzed in the sound level (SPL) tests. The dataset comprises 1 499 measurements. The arithmetic mean thrust for this range was 211.21 N. This resulted from a longer test period and the increased number of the recorded data points. Analysis of the plot shows that the thrust generated by the propeller in this range remains at a significantly higher level than at 3000 RPM. The trace is stable, although small, short-term fluctuations typical for this type of measurement (measurement noise and brief deviations in system operation) are visible. Despite these fluctuations, there are no abrupt drops or surges in thrust that might indicate disturbances in propeller operation or powerplant instability. It is worth noting that the increase in thrust compared to the 3000 RPM range is very clear and confirms the expected dependence of thrust on crankshaft rotational speed (RPM), which is consistent with aerodynamic principles. Figure 10 presents the time history of thrust produced by the Biela 32 × 12 propeller over the rotational-speed range of approximately 4900 to 5050 RPM. Analysis of this characteristic shows that as the rotational speed increases to 5000 RPM, the propeller generates greater thrust compared to the previous RPM ranges. The dataset comprises 1763 measurements. The arithmetic mean thrust for this range was 337.81 N.

The conducted tests make it possible to assess the relationship between the generated thrust and the sound level emitted by the Biela 32 × 12 propeller at different rotational-speed ranges. For each of the analyzed setpoints, i.e. 3000, 4000, and 5000 RPM, both precise thrust measurements and noise levels were obtained, recorded at two measurement positions (L and T) using the Abatronic AB-8852, which also enabled a reliable determination of errors and measurement uncertainties. Analysis of these results indicates that at the lowest RPM both thrust and noise level are at their lowest among all tested ranges.

Compared to 3000 RPM, a clear increase in sound level was observed at both measurement positions (L and T). This confirms the direct relationship between increasing crankshaft speed and the rise in emitted noise level. At the highest crankshaft speed, i.e., 5000 RPM, an average thrust of 337.81 N was obtained from 1,763 measurements, which is more than triple the value at 3000 RPM as well as one and a half times the value at 4000 RPM.

Here, a clear increase in noise relative to 4000 RPM can also be observed: L (MIN) and L (MAX) increased by 7.1 dB and 6.6 dB, respectively, and relative to 3000 RPM by as much as 11.5 dB and 12 dB. At position T, the values increased in this range by nearly 9 dB (MIN) and 7.3 dB (MAX) relative to 3000 RPM. The increase in thrust from 111 N (3000 RPM) to 337.8 N (5000 RPM) causes L (MAX) to rise from 90.5 dB to 102.5 dB (+12 dB). The noise-level increment per 100 N of thrust ranges on the order of ~3.7–5.3 dB, depending on the range and type of measurement. This relationship describes a typical propeller operating characteristic, where an increase in thrust results not only in higher powerplant efficiency, but also in greater noise emission. It is also worth emphasizing that despite the rise in noise level, the obtained thrust traces are stable in each RPM range, which positively affects the repeatability and credibility of the acoustic measurement results. The presented increments and relationships between sound level (noise) and thrust are significant and well exceed the measurement uncertainty.

Sound level measurement for the Falcon 32×13 three-bladed carbon-fiber propeller

The test results for the Falcon 32 × 13 propeller show a clear increase in noise level with increasing rotational speed. At 3000 RPM, the SPL values span 84.4–96.7 dB (L MIN = 89.2, L MAX = 90.5; T MIN = 84.4, T MAX = 96.7; Figure 11). At 4000 RPM they span 99.2–101.9 dB (L MIN ≈ 101.0, L MAX = 101.9; T MIN = 99.2, T MAX ≈ 100.8; Figure 12). At 5000 RPM they range from 104.0 to 109.3 dB (Figure 13). The highest values were always recorded at the highest crankshaft speeds, confirming that noise level (SPL) strongly depends on RPM noise level and on the propeller operating characteristics. The differences between the readings at positions L and T reflect the influence of the measurement location and propeller operating characteristics.

The same sound level meter (Abatronic AB-8852) was used at both positions L and T; therefore, the Type-B uncertainty is identical for both positions (u_B = 0.81 dB). The combined standard uncertainty u_c is generally higher at position T, because the Type-A component is slightly larger there; the only exception is 3000 RPM, where u_c at L is marginally higher (e.g., L MIN 0.95 dB vs T MIN 0.87 dB). Detailed calculations for the Falcon 32 × 13 propeller are given in Table 2. Across all RPM settings, the Type-A standard uncertainty of the mean is small (typically < 0.4 dB), which confirms good repeatability of the measurements. The results shown in Figures 14–16 present the thrust characteristics generated by the propeller over three rotational-speed (RPM) ranges. Each plot demonstrates the stability of the measurements and the thrust values obtained during real engine operation with the tested propeller.

In Figure 14 (range approximately 2900–3100 RPM), the dataset comprises 2 170 measurements. The arithmetic mean thrust for this range was 120.50 N. The thrust trace is fairly stable, without pronounced jumps, although small, random deviations typical of dynamic measurements

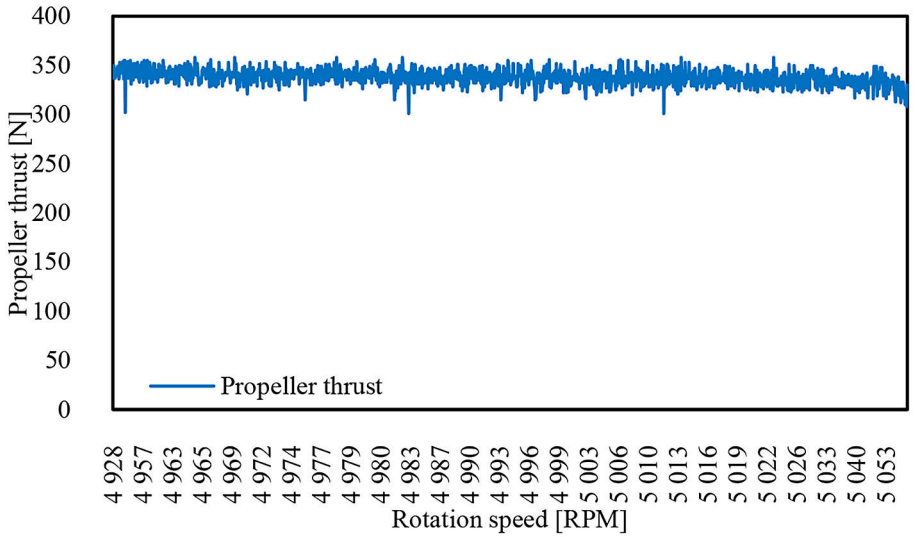

Figure 10. Thrust characteristic of the Biela 32 × 12 propeller for the 4900–5050 RPM range

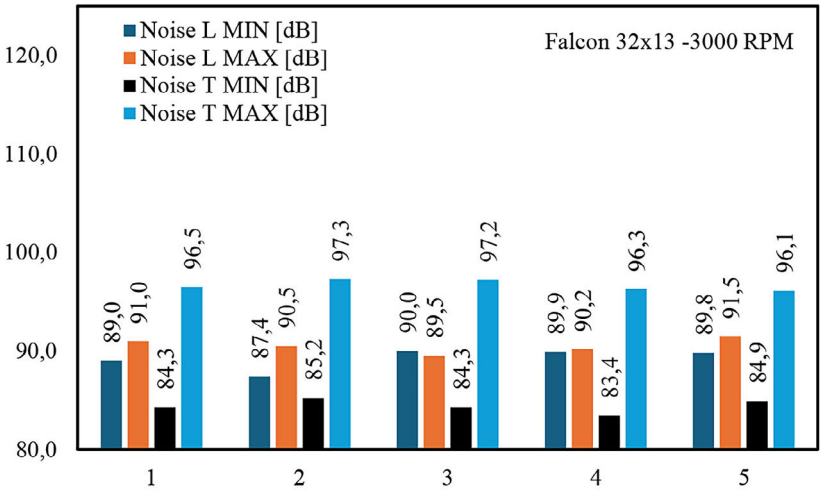

Figure 11. Sound level measurement—minimum and maximum values for the powerplant equipped with the Falcon 32 × 13 propeller, recorded at positions L and T with the Abatronic AB-8852 at 3000 RPM

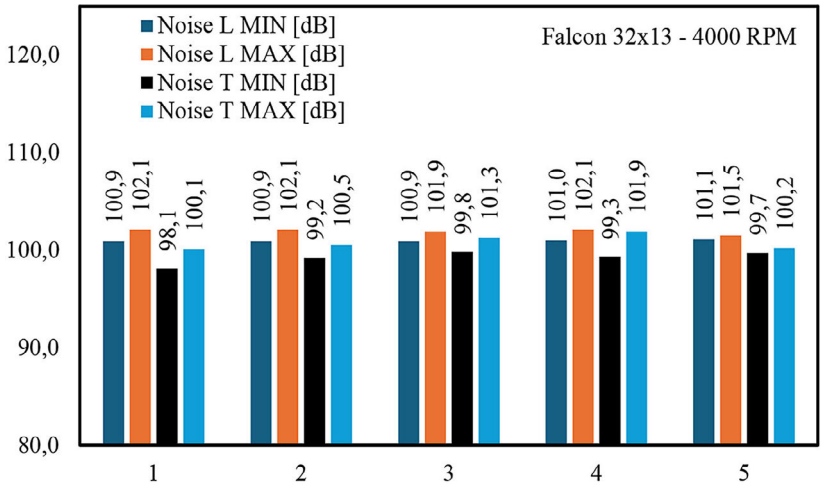

Figure 12. Sound level measurement—minimum and maximum values for the powerplant equipped with the Falcon 32 × 13 propeller, recorded at positions L and T with the Abatronic AB-8852 at 4000 RPM

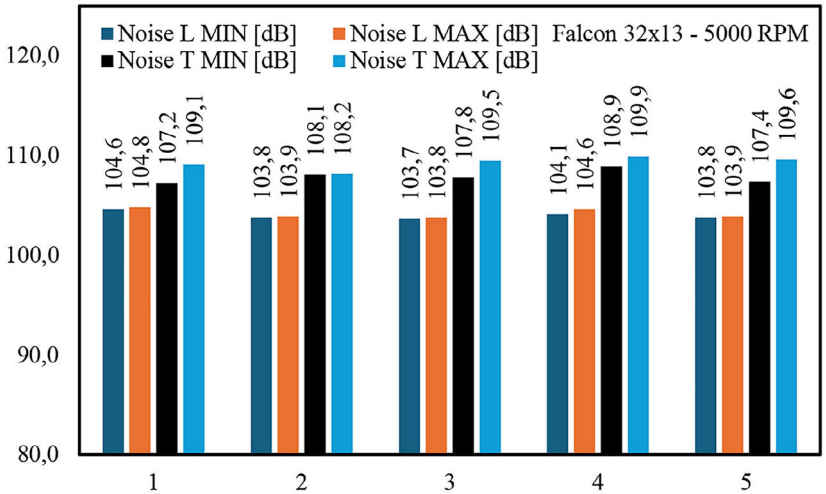

Figure 13. Sound level measurement—minimum and maximum values for the powerplant equipped with the Falcon 32 × 13 propeller, recorded at positions L and T with the Abatronic AB-8852 at 5000 RPM

Table 2. Results of measurement error and measurement uncertainty calculations for the Falcon 32 × 13 propeller

Results for the Falcon 32 × 13 propeller – 3000 RPM				
Measurement type	Mean value	Measurement error / Type A uncertainty u_A [dB]	Type B uncertainty u_B [dB]	Combined uncertainty u_C [dB]
Noise L MIN	89.2	0.49	0.81	0.95
Noise L MAX	90.5	0.34	0.81	0.88
Noise T MIN	84.4	0.31	0.81	0.87
Noise T MAX	96.7	0.24	0.81	0.84
Results for the Falcon 32 × 13 propeller – 4000 RPM				
Measurement type	Mean value	Measurement error / Type A uncertainty u_A [dB]	Type B uncertainty u_B [dB]	Combined uncertainty u_C [dB]
Noise L MIN	101.0	0.04	0.81	0.81
Noise L MAX	101.9	0.12	0.81	0.82
Noise T MIN	99.2	0.30	0.81	0.86
Noise T MAX	100.8	0.35	0.81	0.88
Results for the Falcon 32 × 13 propeller – 5000 RPM				
Measurement type	Mean value	Measurement error / Type A uncertainty u_A [dB]	Type B uncertainty u_B [dB]	Combined uncertainty u_C [dB]
Noise L MIN	104.0	0.16	0.81	0.82
Noise L MAX	104.2	0.21	0.81	0.83
Noise T MIN	107.9	0.30	0.81	0.86
Noise T MAX	109.3	0.29	0.81	0.86

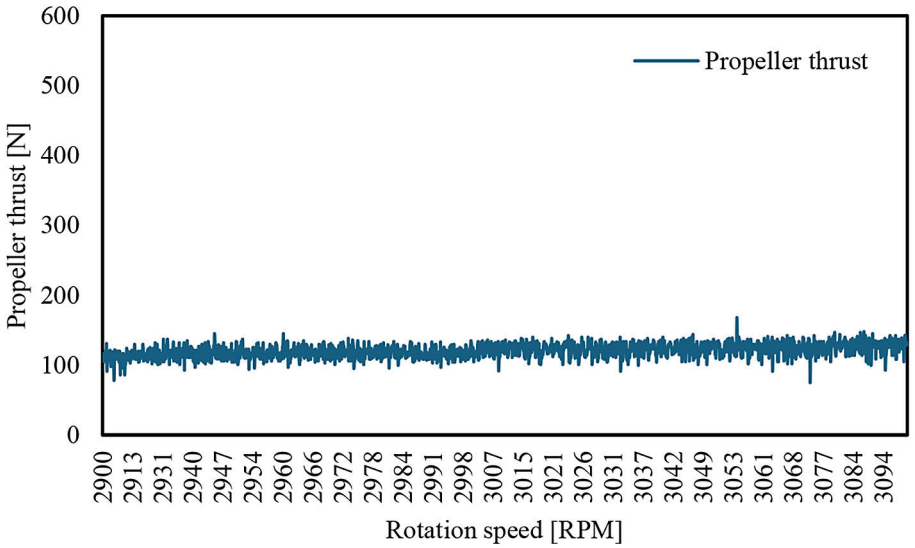

Figure 14. Thrust characteristic of the Falcon 32 × 13 propeller for the 2900–3100 RPM range

under laboratory conditions are visible. The mean thrust increases gradually along with crankshaft rotational speed.

Figure 15 shows the thrust characteristic for the 3900–4100 RPM range. The plot is based on 1098 measurement results. The arithmetic mean thrust for this RPM range was 190.06 N. Despite occasional, short-term fluctuations, the plot indicates high repeatability over the course of the test and an absence of abrupt disturbances in system operation. The upward trend relative to the previous range is clear, and the higher engine power enables the same propeller to produce greater thrust.

In Figure 16, for the ~4900–5020 RPM range, the arithmetic mean from 639 measurements was 322.78 N. The trace confirms powerplant stability even at high rotational speeds, though short-term drops and rises in thrust are visible. The mean thrust clearly exceeds the values from the lower RPM ranges. When analyzing the measurement

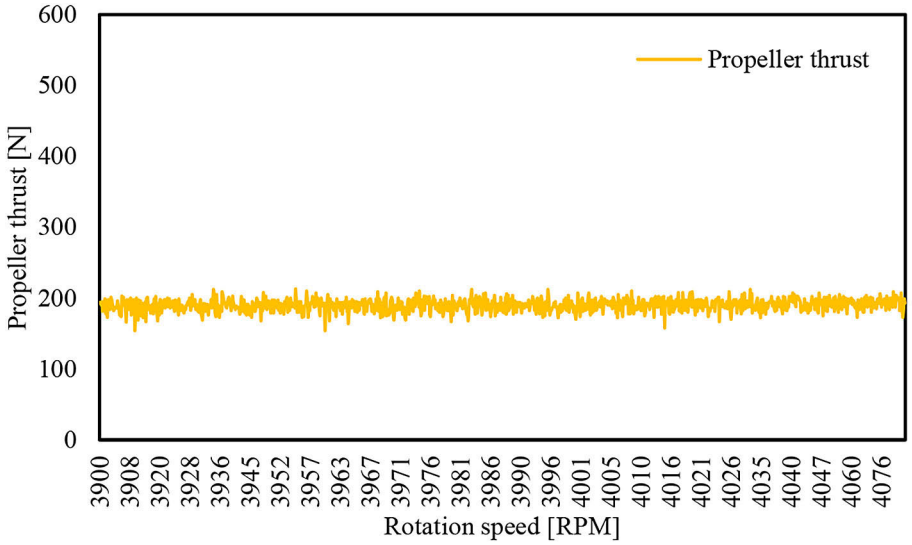

Figure 15. Thrust characteristic of the Falcon 32 × 13 propeller for the 3900–4100 RPM range

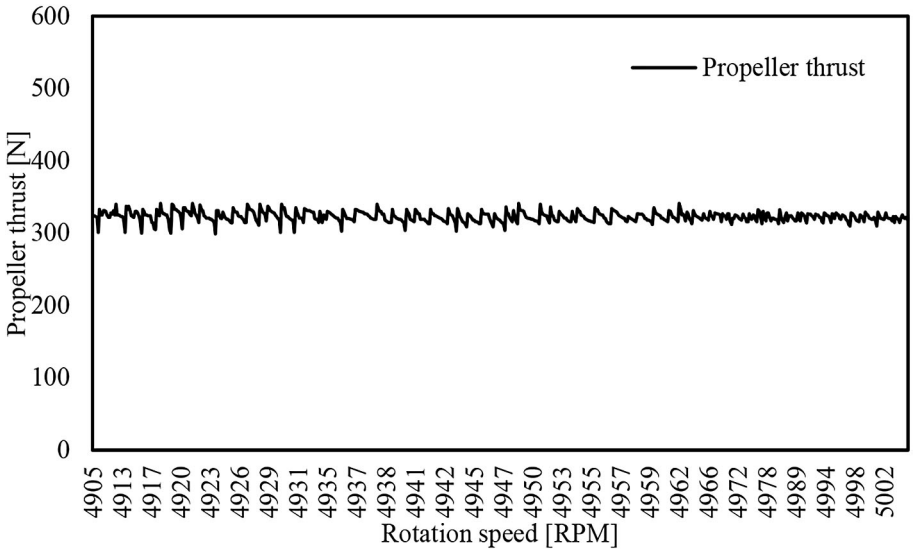

Figure 16. Thrust characteristic of the Falcon 32 × 13 propeller for the 4900–5020 RPM range

results for the Falcon 32 × 13 propeller in three crankshaft RPM ranges, a clear correlation can be observed between increasing thrust and the rise in the generated noise level. In the lowest RPM range (2900–3100 RPM), the mean thrust was 120.50 N, and the noise level recorded at positions L and T was in the 89.2–96.6 dB band. In the next range (3900–4100 RPM), a significant increase was recorded the mean thrust reached 190.06 N, and the noise level rose to 98.6–101.9 dB. The highest values were noted in the 4900–5020 RPM interval, where the mean thrust was 322.78 N, and the recorded noise level reached up to 109.3 dB. This relationship is particularly evident when comparing changes: increasing RPM from 3000 to 5000 (≈+67%) raised thrust by ≈2.7× (from ~120 N to >320 N). Over the same range, the SPL increased by 14.8 dB (L MIN) and 13.7 dB (L MAX); at position T, it increased by 23.5 dB (T MIN) and 12.6 dB (T MAX). This means that each subsequent increase in powerplant output and generated thrust entails a rise in sound emission, significant for user comfort and environmental constraints.

Sound level measurement for the Biela 32×14 three-bladed carbon-fiber propeller

The measurement results for the Biela 32×14 propeller show a clear, systematic increase in sound level with increasing RPM. At 3000 RPM, position L spans 88.1–90.9 dB, and position T spans 92.0–94.9 dB (Figure 17). At 4000 RPM,

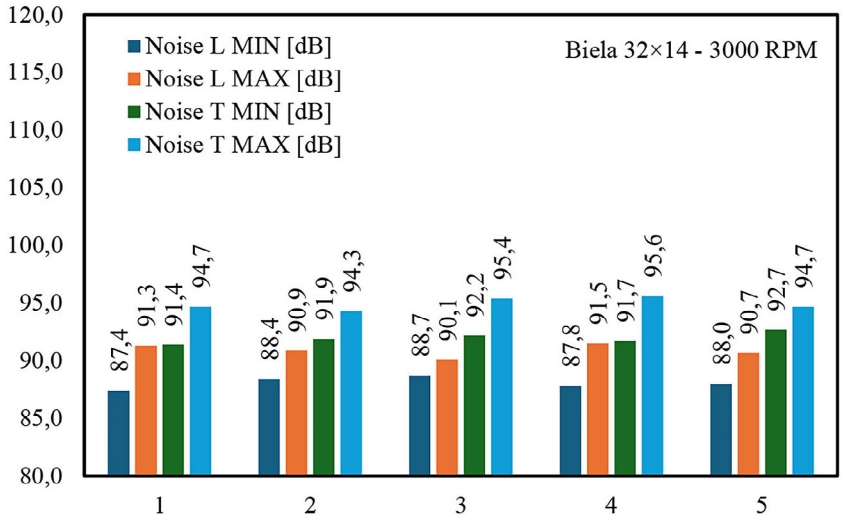

Figure 17. Sound level measurement—minimum and maximum values for the powerplant equipped with the Biela 32 × 14 propeller, recorded at positions L and T with the Abatronic AB-8852 at 3000 RPM

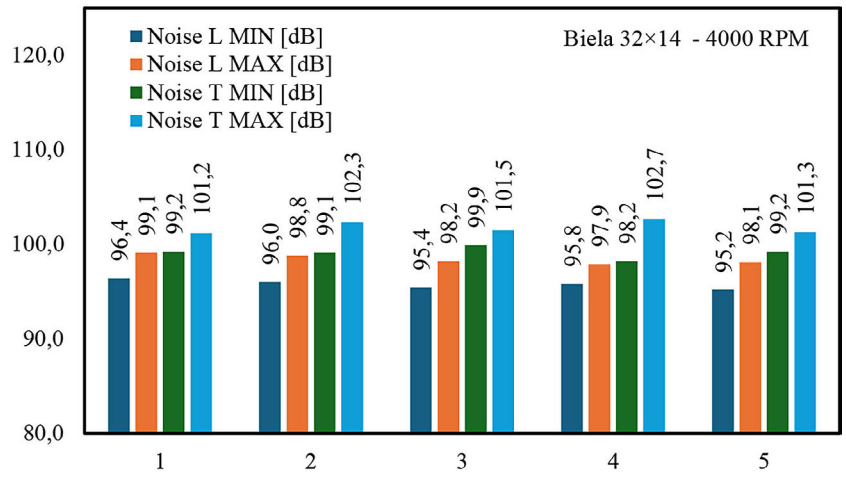

Figure 18. Sound level measurement—minimum and maximum values for the powerplant equipped with the Biela 32 × 14 propeller, recorded at positions L and T with the Abatronic AB-8852 at 4000 RPM

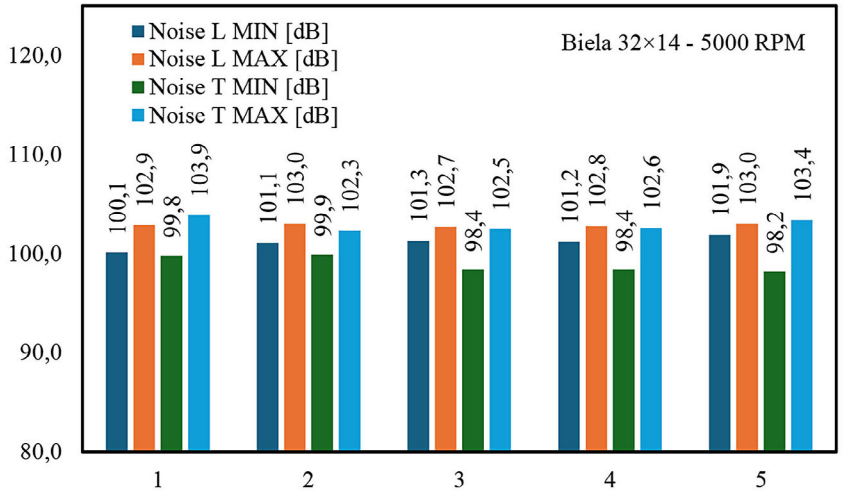

Figure 19. Sound level measurement—minimum and maximum values for the powerplant equipped with the Biela 32 × 14 propeller, recorded at positions L and T with the Abatronic AB-8852 at 5000 RPM

L spans 95.8–98.4 dB and T spans 99.1–101.8 dB (Figure 18). At 5000 RPM, L spans 101.1–102.9 dB, while T spans 98.9–102.9 dB (Figure 19). From 3000 to 4000 RPM the SPL increases by about +7–8 dB (depending on metric), and from 4000 to 5000 RPM by +1–5 dB; over 3000→5000 RPM the total increase is +13.0 dB (L MIN), +12.0 dB (L MAX), +6.9 dB (T MIN) and +8.0 dB (T MAX). This indicates a strong dependence of sound level not only on the aerodynamic characteristics of the propeller, but also on the dynamics of the entire powerplant. The results show that increasing shaft power and thus generated thrust produces a significant rise in noise emission.

The same sound level meter (Abatronic AB-8852) was used at both positions, so the Type-B uncertainty is identical for L and T (u_B = 0.81). The Type-A component is small and the combined standard uncertainty is in the 0.81–0.89 dB range depending on RPM and metric. Detailed values are given in Table 3. The analysis of the presented propeller thrust plots over three rotational-speed (RPM) ranges clearly shows the effect of increasing RPM on the generated thrust. In the lowest crankshaft speed range (approx. 2900–3100 RPM), the arithmetic mean thrust was 147.04 N, and its trace remained stable. This dataset was compiled from 2 482 measurements (Figure 20). In the 3900–4100 RPM range, the arithmetic mean thrust was 272.88 N. The thrust time history for this RPM range was produced on the basis of 1 505 measurements recorded by the test-stand instrumentation (Figure 21). At the highest rotational-speed range (4900–5000 RPM), the arithmetic mean thrust reached 405.48 N (Figure 22). The thrust characteristic for this engine RPM range was derived from 228 measurements. The trace remains smooth, confirming proper and stable operation of the powerplant even under extreme conditions. The increase in thrust along with crankshaft rotational speed is clearly linear and well visible on all three plots, which is consistent with aerodynamic principles for this type of propulsion system. The obtained values show how significantly increasing rotational speed affects propeller efficiency, enabling progressively greater thrust in successive operating ranges. The recording of these measurements serves as a reference for sound-level (SPL) measurements for the given test ranges and provides a general overview of the phenomena presented.

Comparison of propeller variants – sound level and thrust as a function of rotational speed

The results unambiguously confirm a strong, monotonic dependence of noise level and thrust on engine crankshaft RPM. For all three propellers

Table 3. Results of measurement error and measurement uncertainty calculations for the Biela 32 × 14 propeller

Results for the Biela 32 × 14 propeller – 3000 RPM				
Measurement type	Mean value	Measurement error / Type A uncertainty u_A [dB]	Type B uncertainty u_B [dB]	Combined uncertainty u_C [dB]
Noise L MIN	88.1	0.23	0.81	0.84
Noise L MAX	90.9	0.25	0.81	0.85
Noise T MIN	92.0	0.22	0.81	0.84
Noise T MAX	94.9	0.24	0.81	0.85
Results for the Biela 32 × 14 propeller – 4000 RPM				
Measurement type	Mean value	Measurement error / Type A uncertainty u_A [dB]	Type B uncertainty u_B [dB]	Combined uncertainty u_C [dB]
Noise L MIN	95.8	0.21	0.81	0.84
Noise L MAX	98.4	0.23	0.81	0.84
Noise T MIN	99.1	0.27	0.81	0.85
Noise T MAX	101.8	0.30	0.81	0.86
Results for the Biela 32 × 14 propeller – 5000 RPM				
Measurement type	Mean value	Measurement error / Type A uncertainty u_A [dB]	Type B uncertainty u_B [dB]	Combined uncertainty u_C [dB]
Noise L MIN	101.1	0.29	0.81	0.86
Noise L MAX	102.9	0.06	0.81	0.81
Noise T MIN	98.9	0.37	0.81	0.89
Noise T MAX	102.9	0.30	0.81	0.87

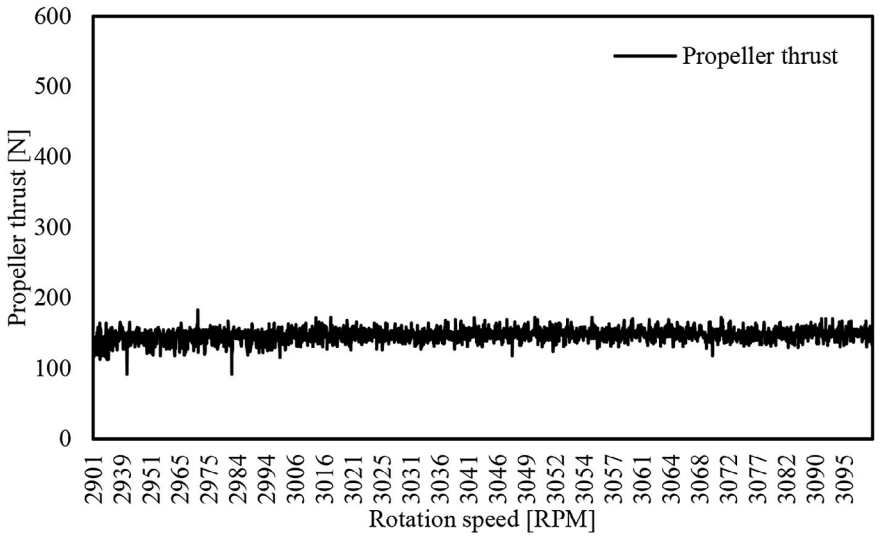

Figure 20. Thrust characteristic of the Biela 32 × 14 propeller for the 2900–3100 RPM range

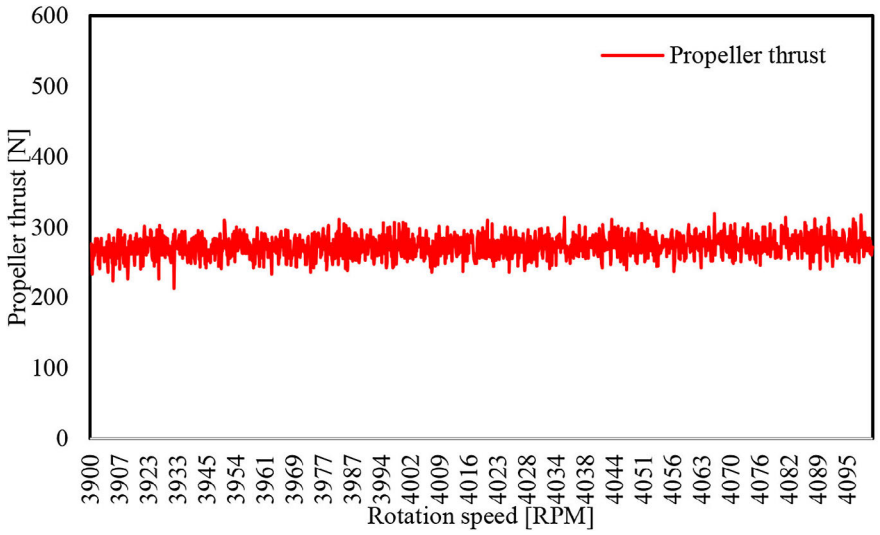

Figure 21. Thrust characteristic of the Biela 32 × 14 propeller for the 3900–4100 RPM range

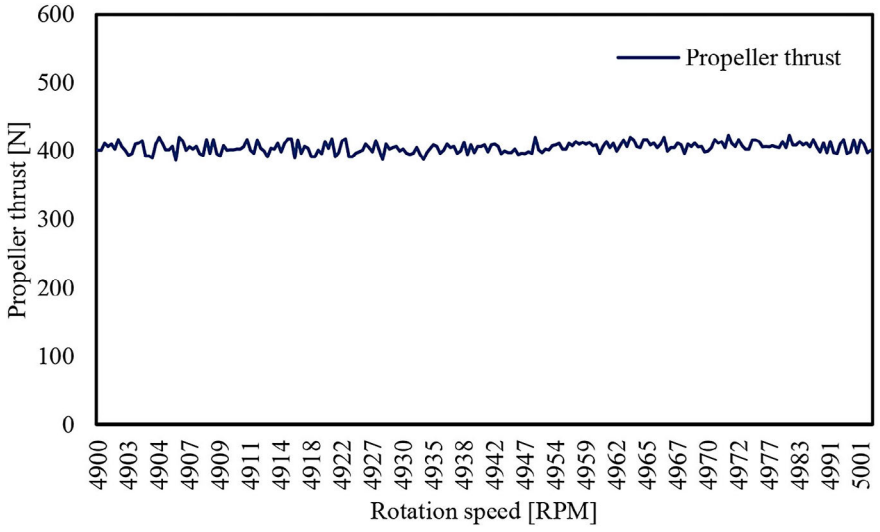

Figure 22. Thrust characteristic of the Biela 32 × 14 propeller for the 4900–5000 RPM range

(Biela 32 × 12, Falcon 32 × 13, Biela 32 × 14), increasing from 3000 to 5000 RPM resulted in a significant rise in both the recorded sound levels and the generated thrust. For example, for the Biela 32 × 12 propeller, mean L(MAX) values increased from approximately 90.7 dB (3000 RPM) to 102.5 dB (5000 RPM), with the average thrust rising concurrently from 111.0 N to 337.8 N. The order of magnitude of the noise increase (≈ +12 dB) is consistent with the parallel increase in aerodynamic blade loading and blade tip speeds, which dominate the acoustic emission mechanism of the propeller. In the lower RPM range, the spread of sound levels measured at position L was small: Biela 32 × 12 (L: 88.5–90.7 dB), Falcon 32 × 13 (L: 89.2–90.5 dB), Biela 32 × 14 (L: 88.1–90.9 dB). At the same time, thrust differed: 111.0 N (Biela 32 × 12), 120.5 N (Falcon 32 × 13), and 147.0 N (Biela 32 × 14). This means that, at a similar noise level, the higher-pitch propeller (32 × 14) provided noticeably higher thrust at 3000 RPM. Data from position T (aft of the aircraft tail) fell within a similar range (e.g., 92.0–94.9 dB for Biela 32 × 14), confirming consistency of the results in the low RPM range.

In the mid-RPM range, more pronounced acoustic differences between propeller variants began to appear. The Falcon 32 × 13 was clearly louder in the disk plane: 101.0–101.9 dB (L), while Biela 32 × 12 reached 93.6–95.9 dB (L) and Biela 32×14 95.8–98.4 dB (L). Concurrently, thrust was: 211.2 N (Biela 32 × 12), 190.1 N (Falcon 32 × 13), and 272.9 N (Biela 32 × 14). From a thrust/noise trade-off perspective, the Biela 32 × 14 is the best variant (higher thrust than the other two while having lower L(MAX) than the Falcon 32 × 13). In the aft measurement (T), the Falcon reached 99.2–100.8 dB, and Biela 32 × 14 up to 101.8 dB, suggesting directionality effects and a somewhat different characteristic for the respective blade profiles.

At the highest RPM, all propellers produced >100 dB sound levels. In the disk plane, L(MAX) was: 102.5 dB (Biela 32 × 12), 104.2 dB (Falcon 32 × 13), and 102.9 dB (Biela 32 × 14). In the aft position, T(MAX) recorded: 104.5 dB (Biela 32 × 12), 109.3 dB (Falcon 32 × 13), and 102.9 dB (Biela 32 × 14). The Falcon 32 × 13 therefore produced the highest noise level at 5000 RPM, particularly in the exhaust/wake direction (T), which may result from a combination of geometry, pitch, and tip-speed distribution. At the same time, Biela 32 × 14 delivered the highest thrust (405.5 N), clearly exceeding Biela 32 × 12 (337.8 N) and Falcon 32 × 13 (322.8 N), with the L and T noise levels similar to Biela 32 × 12 and decidedly lower than Falcon 32 × 13 (T). From a practical standpoint, the 32 × 14 variant therefore offers the most favorable noise–thrust compromise at 5000 RPM.

Figure 23 compares mean sound levels as a function of RPM for all three propellers and both microphone locations. A clear upward trend is visible across 3000–5000 RPM. In the propeller disk plane (L), the mean maximum levels at 5000 RPM are 102.5 dB (Biela 32 × 12), 104.2 dB (Falcon 32 × 13), and 102.9 dB (Biela 32 × 14). In the aft position (T), the corresponding mean maxima are 104.5 dB, 109.3 dB, and 102.9 dB, respectively, indicating stronger downstream directivity for the

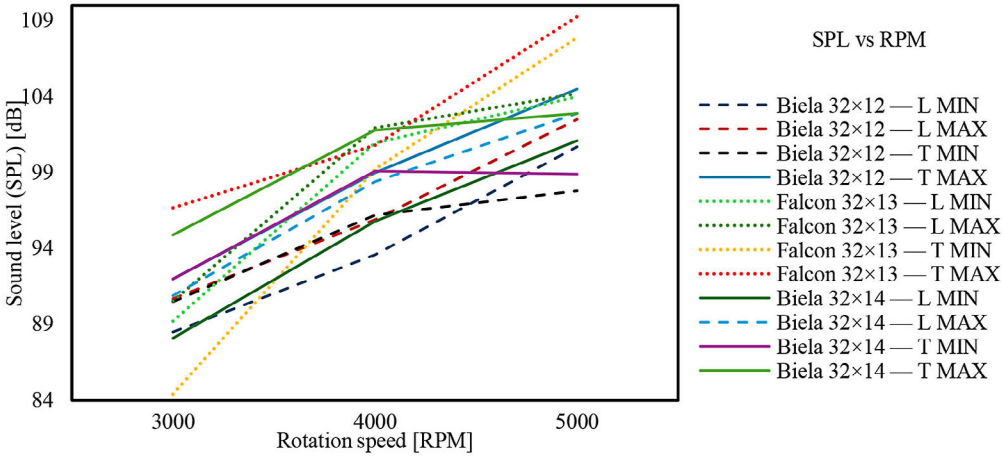

Figure 23. Sound pressure level as a function of rotational speed — mean minimum and maximum values at two microphone locations (in the propeller disk plane and behind the tail) for the Biela 32 × 12, Falcon 32 × 13, and Biela 32 × 14 propellers (Abatronic AB-8852)

Falcon at high RPM. Real-world audibility (rule-of-thumb). Assuming free-field spherical spreading without ground or atmospheric absorption, the detection range can be estimated by [35]:

$$L_p(r) = L_p(r_0) - 20log_{10}\left(\frac{r}{r_0}\right) \quad (7)$$

where: $L_p(r)$ – sound pressure level at distance rrr from the source [dB], $L_p(r_0)$ – sound pressure level at the reference distance r_0 [dB], r – distance from the source [m], r_0 – reference distance (measurement point of known level) [m], $log_{10}(\cdot)$ – base-10 logarithm, coefficient 20 – arises from the inverse-distance law for pressure levels in a free field (spherical spreading).

Using the aft position T as the reference (r_0 = 2.79 m), the mean maxima at 5000 RPM translate approximately to: Biela 32 × 14 T(MAX) = 102.9 dB → ~78 dB at 50 m, ~72 dB at 100 m, ~66 dB at 200 m; Falcon 32 × 13 T(MAX) = 109.3 dB → ~84 dB at 50 m, ~78 dB at 100 m, ~72 dB at 200 m. Using position L as the reference (r_0 = 3.0 m), the mean maxima at 5000 RPM translate approximately to: Biela 32 × 14 L(MAX) = 102.9 dB → ~78 dB at 50 m, ~72 dB at 100 m, ~66 dB at 200 m; Falcon 32 × 13 L(MAX) = 109.3 dB → ~85 dB at 50 m, ~79 dB at 100 m, ~73 dB at 200 m. These values are indicative and scenario-dependent (background noise, wind, ground effects), but they provide a practical sense of acoustic footprint based on the conducted measurements. Figure 24 shows mean thrust versus RPM. Qualitatively, the obtained static SPL maxima exceed typical values reported for small electric multirotor UAS due to larger disk loading and the presence of ICE intake/exhaust contributions [6-8]. A rigorous cross-system comparison is beyond our scope here and would require harmonized distances and operating points; nevertheless, the relative differences within our dataset remain valid across scenarios. Biela 32 × 14 consistently delivers the highest thrust at each setpoint (≈147 N at 3000 RPM, ≈273 N at 4000 RPM, ≈405 N at 5000 RPM), followed by Falcon 32 × 13 (≈121 / 190 / 323 N) and Biela 32 × 12 (≈111 / 211 / 338 N). Combined with Figure 23, this highlights that the 32 × 14 propeller offers the most favorable thrust-to-noise trade-off, especially above 4000 RPM.

Operational conclusions

For the Biela 32 × 12 propeller, the increase of L(MAX) from 90.7 to 102.5 dB is about +11.8 dB with the mean thrust rising from 111.0 to 337.8 N (+226.8 N), which corresponds to ~5.2 dB per 100 N. For the Falcon 32 × 13 propeller, the relation between 3000 and 5000 RPM (L(MAX): 90.5 → 104.2 dB; +13.7 dB; thrust: 120.5 → 322.8 N; +202.3 N) is ~6.8 dB per 100 N, indicating less favorable operational performance relative to thrust increase. For the Biela 32 × 14 (L(MAX): 90.9 → 102.9 dB; +12.0 dB; thrust: 147.0 → 405.5 N; +258.5 N) this index is ~4.6 dB per 100 N – the best among the compared configurations. From an operational standpoint (e.g., operations in built-up areas or combat UAS operations), selecting the Biela 32 × 14 propeller allows higher thrust with a lower sound

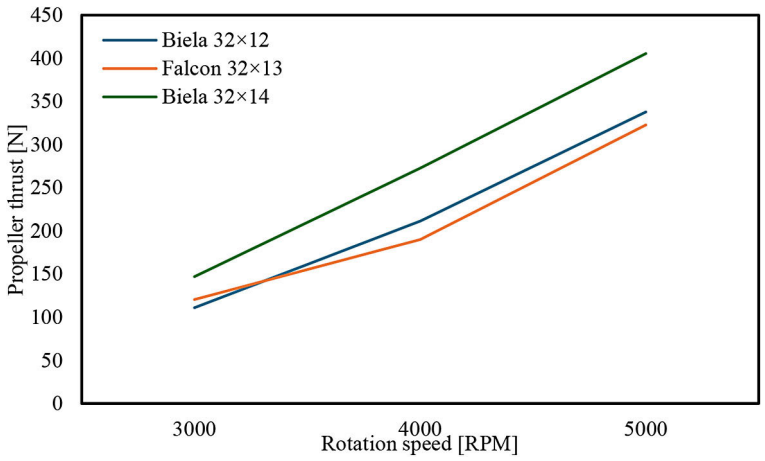

Figure 24. Propeller thrust as a function of rotational speed — mean values for Biela 32 × 12, Falcon 32 × 13, and Biela 32 × 14

level per unit thrust increment than in the case of the Falcon 32 × 13.

Noise-abatement options and next steps

On the basis of the obtained results, practical levers include:

- RPM management (operate at or below 4000 RPM when mission requirements allow);
- propeller selection with a more favorable thrust-to-noise index (e.g., Biela 32 × 14 in our tests);
- geometric refinements (moderate pitch/radial pitch distribution; swept/scimitar tips; hub fairings) aimed at reducing tip and broadband components;
- engine-borne noise mitigation (intake/exhaust muffling, compliant mounts, local acoustic liners);
- propulsive gearing or variable-pitch control to maintain lower blade-tip Mach number at required thrust. In a follow-on campaign we plan to include octave-band/BPF diagnostics to decompose sources (engine core vs. propeller) and quantify their operational relevance across flight regimes.

Measurement differences between positions (L and T) and directivity of noise emission

The results showed consistent, though not identical, tendencies between the two microphone positions: position L (3 m from the propeller axis in the propeller-disk plane) and position T (aft of the fuselage, 2.6 m behind the propeller, with lateral offset). Higher values for the Falcon propeller in the T position at 5000 RPM (T(MAX) 109.3 dB) suggest a stronger downstream (wake/exhaust) noise component relative to the other propellers, which may result from a different tip-loading distribution and interaction with the propeller slipstream. At the same time, local anomalies (e.g., sporadically lower T(MIN) at higher RPM relative to 4000 RPM for some configurations) should be associated with a different source directivity and sensitivity differences, not with a reversal of the general RPM–noise relationship. The measurement arrangement defined in the work and the fixed distances increase data comparability, but they do not entirely eliminate directional effects, which can be significant for propellers. A slight decrease of T(MIN) from 99.1 dB (4000 RPM) to 98.9 dB (5000 RPM) lies within the combined uncertainty (≈0.89 dB) and reflects source directivity rather than a reversal of the RPM-noise trend.

Thrust/noise efficiency with respect to crankshaft speed

At 4000 RPM, the Biela 32 × 14 propeller achieved 272.9 N at L(MAX) = 98.4 dB, whereas the Falcon 32 × 13 produced 190.1 N at L(MAX) = 101.9 dB. This means that at this operating point the Biela 32 × 14 generated substantially higher thrust (~+43%) and a decidedly lower sound level (−3.5 dB in the disk plane) than the Falcon propeller. At 5000 RPM the Biela 32 × 14 maintained its advantage in thrust production (405.5 N), while the Falcon 32 × 13 produced an aft sound level T(MAX) of 109.3 dB compared with 102.9 dB. The Biela 32 × 12 propeller offers a compromise between moderate noise and medium thrust (e.g., 337.8 N at L(MAX) = 102.5 dB in the disk plane). These relations are particularly important for powerplant (engine–propeller) selection when the goal is noise minimization while maintaining the required thrust margin.

From an aerodynamic standpoint, the larger pitch of the Biela 32 × 14 allows, at a given RPM, a greater pressure differential and higher thrust, often at a slightly lower tip speed for the same useful power in flight. Under static conditions (test stand), however, tip loading increases and the risk of increased broadband (turbulent) components rises. Nevertheless, empirically the Biela 32 × 14 proved more acoustically efficient than the Falcon 32 × 13 (lower dB/100 N dependence), which suggests a more favorable combination of airfoil profile and radial pitch distribution. Conversely, the higher sound levels of the Falcon 32 × 13 – especially “behind the propeller” at 5000 RPM – may indicate stronger noise modulation by the primary vortex and tip components, which radiate directionally toward the observer aft of the aircraft. This hypothesis is reinforced by the L vs. T differences and their magnitude at high RPM.

CONCLUSIONS

Among the configurations tested, the best thrust/noise compromise was demonstrated by the Biela 32 × 14 propeller especially at crankshaft speeds of 4000–5000 RPM. The Biela 32 × 12

propeller remains a sensible choice when noise reduction is prioritized at the expense of a possible decrease in thrust margin. The Falcon 32 × 13 propeller, despite good thrust parameters, exhibits the least favorable noise-emission profile at high RPM, particularly in the downstream (slipstream/exhaust) direction. Taking account of measurement uncertainties and the test-stand geometry, these conclusions provide practical guidance for selecting a propeller for two-stroke powerplants of ultralight aircraft operating in acoustically sensitive conditions. This is particularly important when selecting propeller airfoils for the aircraft intended for military (combat) purposes or for civil aircraft flying in natural areas or populated regions:

- sound level increases with crankshaft RPM. Across 3000–5000 RPM the sound level increases by ~7–24 dB depending on the metric and propeller; e.g., for Biela 32 × 12, L(MAX) rises from about 90.7 to 102.5 dB;
- thrust and sound level are interdependent. The sound level increases along with thrust. For Biela 32 × 12, the sound-level increment per approximately 100 N of thrust is about 3.7–5.3 dB, and the thrust traces are stable across the entire RPM range;
- the best effectiveness between thrust and generated sound level during the tests was provided by the Biela 32 × 14 propeller; it achieves the highest thrust in every band (≈147 N at 3000 RPM, ≈273 N at 4000 RPM, ≈405 N at 5000 RPM) with L(MAX) ≈ 90.9 / 98.4 / 102.9 dB. The Falcon 32 × 13 shows opposite tendencies, producing the highest sound levels aft of the propeller (T(MAX) up to 109.3 dB at 5000 RPM). The Biela 32 × 12 represents a compromise, generating moderate thrust with concurrent noise emission;
- noise emission is directional and depends on propeller configuration. The differences between measurement in the propeller-disk plane (L) and aft of the propeller (T) are pronounced, especially for the Falcon 32 × 13. This propeller is relatively louder in the downstream direction at high RPM, which is operationally significant in terms of impact on the environment behind the aircraft.

Key practical implications:

- for the operations near populated or environmentally sensitive areas, the Biela 32 × 14 is preferred: at 5000 RPM it delivers higher thrust (≈405 N) with a substantially lower aft SPL than Falcon 32 × 13 (T(MAX) 102.9 dB vs 109.3 dB, Δ ≈ 6.4 dB);
- keeping RPM at or below 4000 holds mean maximum levels to ≤101.9 dB (L) and ≤101.8 dB (T) for the tested propellers, providing a practical operational setpoint when noise limits apply, while still delivering ≈190–273 N thrust depending on the propeller.

If further noise reduction is required, evaluate octave-band diagnostics and tip-speed management first; both target the dominant sources without compromising thrust as much as large prop changes would.

The results were obtained under static conditions, with controlled auxiliary cooling and fixed, discrete RPM setpoints. In aircraft flight, the acoustic characteristics may change (interaction with the incoming flow, different local Mach numbers at the tips, influence of fuselage/wing). The use of additional instrumentation (spectral analysis, BPF and harmonics) would make it possible to distinguish the contribution of loading noise from tip noise. Moreover, spectral decomposition under varied operating conditions can separate the noise of the engine and its accessories (intake, exhaust, auxiliary cooling) from propeller-borne components, enabling a source-by-source breakdown – an interesting direction for a subsequent study.

REFERENCES

1. Rajpert T. Hałas lotniczy i sposoby jego zwalczania. Warszawa; 1980.
2. Merkisz J, Płotnicka N, Dahlke G. Hałas emitowany przez statki powietrzne o napędzie turbośmigłowym i turbowentylatorowym podczas startu i lądowania. Technika Transportu Szynowego. 2013;(10).
3. Merkisz J, Karpiński D, Galant M, Markowski J. Badanie poziomów dźwięku hałasu lotniczego na obszarach sąsiadujących z portem lotniczym Poznań-Ławica. Technika Transportu Szynowego. 2013;(10).
4. Cieślak S. Analiza możliwości zwiększenia prędkości przelotowej i zmniejszenia poziomu hałasu wiatrakowca. Prace Instytutu Lotnictwa. 2011;219:31–38.
5. Strzelczyk P. Wybrane zagadnienia aerodynamiki śmigieł. Rzeszów: Oficyna Wydawnicza Politechniki Rzeszowskiej; 2011.
6. Schäffer B, Pieren R, Heutschi K, Wunderli JM,

Becker S. Drone noise emission characteristics and noise effects on humans: a systematic review. Int J Environ Res Public Health. 2021;18(11):5940. https://doi.org/10.3390/ijerph18115940

7. Intaratep N, Alexander WN, Devenport WJ, Grace SM, Dropkin A. Experimental study of quadcopter acoustics and performance at static thrust conditions. In: 22nd AIAA/CEAS Aeroacoustics Conference; 2016 May 30–Jun 1; Lyon, France.
8. Heutschi K, Ott B, Nussbaumer T, Wellig P. Synthesis of real-world drone signals based on lab recordings. Acta Acustica. 2020;4(6):24.
9. Miedema HME, Oudshoorn CGM. Annoyance from transportation noise: relationships with exposure metrics DNL and DENL and their confidence intervals. Environ Health Perspect. 2001;109(4):409–416.
10. Załącznik nr 16 do Konwencji o międzynarodowym lotnictwie cywilnym, sporządzony w Chicago dnia 7 grudnia 1944 r. Chicago; 1944 Dec 7.
11. Leśko M, Pasek M. Porty lotnicze: wybrane zagadnienia inżynierii ekologicznej. Gliwice: Wydawnictwo Politechniki Śląskiej; 1997.
12. Wróblewski P, Bratkowski P, Borcuch D, Kiszkowiak Ł. Prototype test stand for an aircraft piston engine for testing propeller profiles and advanced materials. Combustion Engines; 2025. https://doi.org/10.19206/CE-204319
13. Balicki W, Kawalec K, Pągowski T, Szczeciński J, Szczeciński S. Historia i perspektywy rozwoju napędów lotniczych. Warszawa: Biblioteka Naukowa Instytutu Lotnictwa; 2005.
14. Brusow W. Optymalne projektowanie wielozadaniowych statków latających. Biblioteka Naukowa Instytutu Lotnictwa; 1996.
15. Kozakiewicz A, Mrozek B. Analiza podstawowych parametrów silników samolotów skróconego startu i lądowania. In: Zbiór prac VI Międzynarodowej Konferencji Naukowo-Technicznej „CRASS 2005"; 2005; Kraków.
16. Olejnik A, Kiszkowiak Ł, Dziubiński A. Aerodynamic analysis of General Aviation airplanes using computational fluid dynamics methods [Badania aerodynamiczne samolotów klasy General Aviation z wykorzystaniem metod numerycznej mechaniki płynów]. Mechanik. 2017;90(8–9):802–804. https://doi.org/10.17814/mechanik.2017.8-9.118
17. Olejnik A, Dziubiński A, Kiszkowiak Ł. CFD simulation of engine nacelle cooling on pusher configuration aircraft. Aircraft Eng Aerosp Technol. 2021;93(9):1421–1429. https://doi.org/10.1108/AEAT-12-2020-0290
18. Olejnik A, Kiszkowiak Ł, Rogólski R, Chmaj G, Radomski M, Majcher M, Omen Ł. The use of unmanned aerial vehicles in remote sensing systems. Sensors. 2020;20:2003. https://doi.org/10.3390/s20072003
19. Wróblewski P. Analysis of torque waveforms in two-cylinder engines for ultralight aircraft propulsion operating on 0W-8 and 0W-16 oils at high thermal loads using the diamond-like carbon composite coating. SAE Int J Engines. 2022;15(1):129–146. https://doi.org/10.4271/03-15-01-0005
20. Wróblewski P, Bratkowski P, Kachel S. Investigation of the influence of propeller blade profile and angle of attack on the performance parameters of an aircraft piston engine. Combustion Engines. https://doi.org/10.19206/CE-208772
21. Zawodny NS, Boyd DD, Burley CL. Acoustic characterization and prediction of representative, small-scale rotary-wing unmanned aircraft system components. In: AHS Annual Forum; 2016. NASA NTRS Doc ID 20160009054.
22. Christian AW, Cabell R. Initial investigation into the psychoacoustic properties of small unmanned aerial system noise. In: 23rd AIAA/CEAS Aeroacoustics Conference; 2017 Jun 5–9; Denver, CO. https://doi.org/10.2514/6.2017-4051
23. Zawodny NS, Christian A, Cabell R. A summary of NASA research exploring the acoustics of small unmanned aerial systems. In: 2018 AHS Technical Meeting on Aeromechanics Design for Transformative Vertical Flight; 2018 Jan 16–19; San Francisco, CA, USA. NASA NTRS Doc ID: 20180002208. Report No.: NF1676L-27827.
24. Ramos-Romero C, Green N, Torija AJ, Asensio C. On-field noise measurements and acoustic characterisation of multi-rotor small unmanned aerial systems. *Aerospace Science and Technology*. 2023;141:108537. https://doi.org/10.1016/j.ast.2023.108537
25. Ivošević J, Ganić E, Petošić A, Radišić T. Comparative UAV noise-impact assessments through survey and noise measurements. International Journal of Environmental Research and Public Health. 2021;18(12):6202. https://doi.org/10.3390/ijerph18126202
26. International Organization for Standardization. *ISO 1996-1:2016 Acoustics—Description, measurement and assessment of environmental noise – Part 1: Basic quantities and assessment procedures*. 3rd ed. Geneva: ISO; 2016. (Confirmed 2021).
27. Lotinga MJB, Ramos-Romero C, Green N, Torija AJ. Noise from unconventional aircraft: a review of current measurement techniques, psychoacoustics, metrics and regulation. *Current Pollution Reports*. 2023;9:724–745. https://doi.org/10.1007/s40726-023-00285-4
28. International Electrotechnical Commission. IEC 61672-1:2013 Electroacoustics – Sound level meters – Part 1: Specifications. 2nd ed. Geneva:

IEC; 2013.

29. Brooks TF, Pope DS, Marcolini MA. Airfoil self-noise and prediction. NASA Reference Publication RP-1218. Washington, DC: NASA; 1989.
30. Rizzi SA, Zawodny NS, Pettingill NA. On the use of acoustic wind tunnel data for the simulation of sUAS flyover noise. AIAA Paper 2019-2630; 2019. https://doi.org/10.2514/6.2019-2630
31. Frant M, Kachel S, Maślanka W. Gust modeling with state-of-the-art computational fluid dynamics (CFD) software and its influence on the aerodynamic characteristics of an unmanned aerial vehicle. Energies. 2023;16(19):6847. https://doi.org/10.3390/en16196847
32. Frant M, Kozakiewicz A, Kachel S. Analysis of impact of gust angle and velocity on the position of stagnation point. Advances in Science and Technology Research Journal. 2020;14(4):49–57. https://doi.org/10.12913/22998624/123006
33. Kocjan J, Kachel S, Rogólski R. Parametrization of the main rotor and working environment for different flight conditions – Computational Fluid Dynamics analysis as an application for multidisciplinary optimization. Journal of Theoretical and Applied Mechanics. 2023;61(4):793–805. https://doi.org/10.15632/jtam-pl/171748
34. Kozakiewicz A, Kachel S, Frant M, Majcher M. Intake system performance stability as a function of flow throttling. Energies. 2022;15(17):6291. https://doi.org/10.3390/en15176291
35. Bies, D. A., Hansen, C. H. Engineering Noise Control: Theory and Practice. 4th ed. Abingdon / New York: Spon Press (Taylor & Francis), 2009.
36. Dorozhovets, M.; Warsza, Z. L. Propozycje rozszerzenia metod wyznaczania niepewności wyniku pomiarów wg Przewodnika GUM (1): Uwzględnianie wpływu autokorelacji i nieadekwatności rozkładu wyników obserwacji w niepewności typu A. Pomiary Automatyka Robotyka, 2007, 11(1).
37. Szydłowski, H. Niepewności w pomiarach. Międzynarodowe standardy w praktyce. Poznań: Wydawnictwo Naukowe UAM, 2006.